Hindawi Publishing Corporation
Journal of Aerodynamics
Volume 2014, Article ID 931232, 11 pages
http://dx.doi.org/10.1155/2014/931232

Research Article

Shape Optimization of an Airfoil in Ground Effect for Application to WIG Craft

Yilei He,[1] Qiulin Qu,[2,3] and Ramesh K. Agarwal[1]

[1]*Department of Mechanical Engineering and Materials Science, Washington University in St. Louis, St. Louis, MO 63130, USA*
[2]*Institute of Fluid Mechanics, Beijing Institute of Aeronautics and Astronautics, Beijing 100191, China*
[3]*Washington University in St. Louis, St. Louis, MO 63130, USA*

Correspondence should be addressed to Ramesh K. Agarwal; rka@wustl.edu

Received 31 May 2014; Accepted 19 October 2014; Published 8 December 2014

Academic Editor: Jian-han Liang

This paper employs a multiobjective genetic algorithm (MOGA) to optimize the shape of a widely used wing in ground (WIG) aircraft airfoil NACA 4412 to improve its lift and drag characteristics, in particular to achieve two objectives, that is, to increase its lift and its lift to drag ratio. The commercial software ANSYS FLUENT is employed to calculate the flow field on an adaptive structured mesh generated by ANSYS ICEM software using the Reynolds-Averaged Navier-Stokes (RANS) equations in conjunction with a one equation Spalart-Allmaras (SA) turbulence model. The results show significant improvement in both the lift coefficient and lift to drag ratio of the optimized airfoil compared to the original NACA 4412 airfoil. It is demonstrated that the performance of a wing in ground (WIG) aircraft can be improved by using the optimized airfoil.

1. Introduction

Ground effect is an aerodynamic phenomenon that occurs on an aircraft during take-off and landing when the aircraft is in close vicinity of the ground. The close proximity of the ground alters the flow of air around the wing causing an increase in the lift and a reduction in the induced drag of the wing. Wing in ground effect (WIG) craft is a type of aircraft which takes-off and lands with very small ground clearance compared to other transport aircrafts. WIG craft is more fuel efficient than other general aviation and transport aircrafts and has relatively very short take-off distance [1]. These advantages make WIG craft attractive for many military and civil applications which require take-off and landing from aircraft carriers from and to water surface, respectively. Therefore, it is of interest to optimize airfoils for the wings of WIG craft for superior performnace by increasing lift as well as the lift to drag ratio.

When flying in the proximity of the ground, the flow around an aircraft is forced to be parallel to the ground due to ground effect; thus, the aerodynamics in ground effect is significantly different from that in out of ground effect in unbounded flow. The aerodynamic analysis requires an additional bounday condition to simulate the effect of the ground [2, 3]. In the realm of ground effect aircraft, most studies have focused on two kinds of ground effect—the steady ground effect (SGE) wherein the flying altitude does not vary with time and the dynamic ground effect (DGE) wherein the flying altitude varies continuously with time [4–11]. However, to date, neither SGE nor DGE have considered the airfoil optimization in the presence of ground.

The focus of this paper is on optimization of one of the most well-known airfoil used for wing in ground effect (WIG) craft—the NACA 4412 airfoil. The goal is to optimize the shape of this airfoil by employing a multiobjective genetic algorithm (MOGA) to improve its aerodynamic performance compared to the original NACA 4412 airfoil. The commercially available software ANSYS FLUENT is used for calculation of the flow field using the Reynolds-Averaged Navier-Stokes (RANS) equations in conjunction with a one equation Spalart-Allmaras (S-A) turbulence model. Using MOGA, globally optimal NACA 4412 airfoil shape is obtained for a typical cruising speed and angle of attack. The two optimization objectives are considered—maximization of the

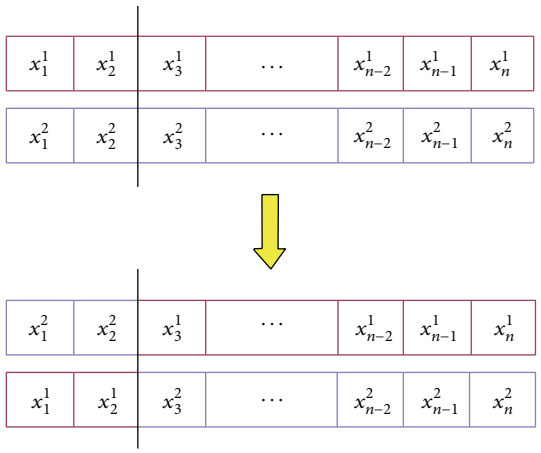

Figure 1: Illustration of the general crossover function in GA.

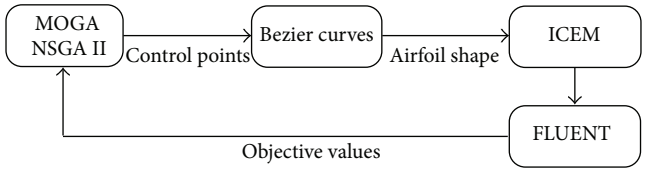

Figure 2: Schematic of information flow in optimization process using MOGA.

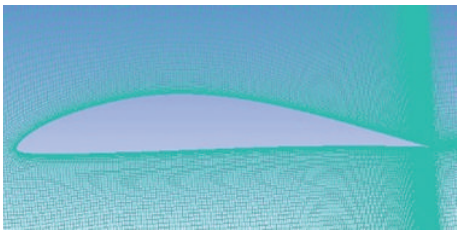

Figure 3: Structured mesh around NACA 4412 airfoil in the presence of ground.

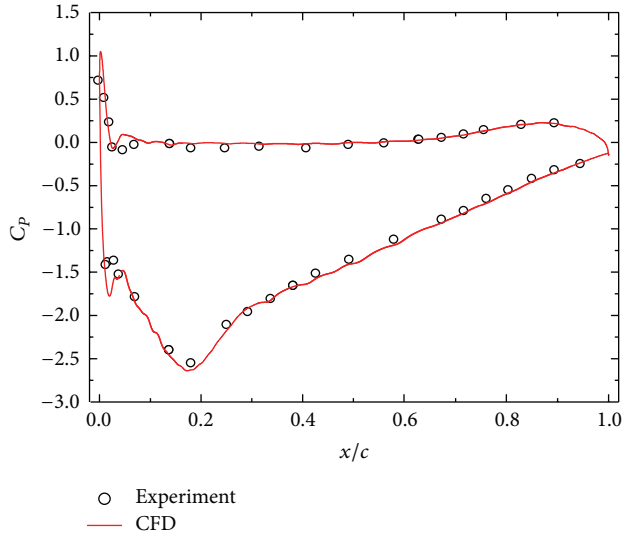

Figure 4: Comparison of computed and experimental pressure coefficient for the Tyrrell-026 airfoil.

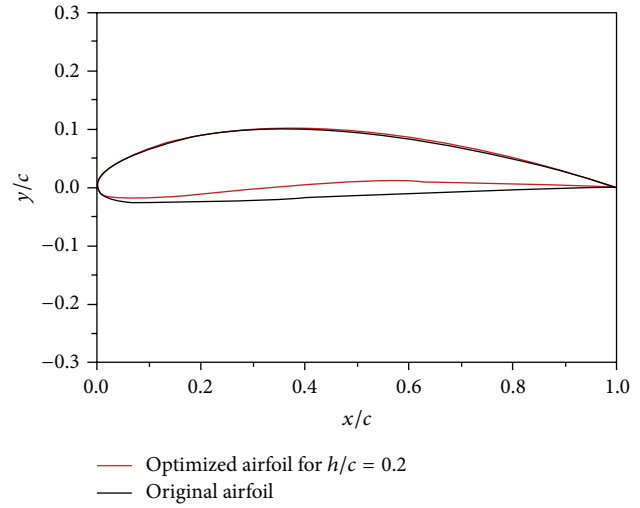

Figure 5: Comparison of shape between the optimized airfoil in ground effect with height above the ground h/c = 0.2 and the original NACA 4412 airfoil.

lift coefficient and the lift to drag ratio. These two parameters are indicators of an aircraft's aerodynamic efficiency. The results for the NACA 4412 airfoil optimized in ground effect are compared with those of the optimized NACA 4412 airfoil in the free stream. This comparison is used to assess what is the best airfoil for WIG craft—the one optimized for ground effect or the one optimized for free-stream. Among various possible heights above the ground, which height can yield the best overall performance for optimization of the airfoil at all heights including the free-stream?

2. Brief Description of the Genetic Algorithm and Airfoil Parameterization

2.1. Single Objective Genetic Algorithm (SOGA). Genetic algorithms are a class of stochastic optimization algorithms inspired by the biological evolution. In GA, a set or generation of input vectors, called individuals, is iterated over, successively combining traits (aspects) of the best individuals until a convergence is achieved. In general, GA employs the following steps [12, 13].

(1) *Initialization*: randomly create N individuals.

(2) *Evaluation*: evaluate the fitness of each individual.

(3) *Natural selection*: remove a subset of the individuals. Often the individuals that have the lowest fitness are removed; although culling, the removing of those individuals with similar fitness, is sometimes performed.

(4) *Reproduction*: pick pairs of individuals to produce an offspring. This is often done by roulette wheel

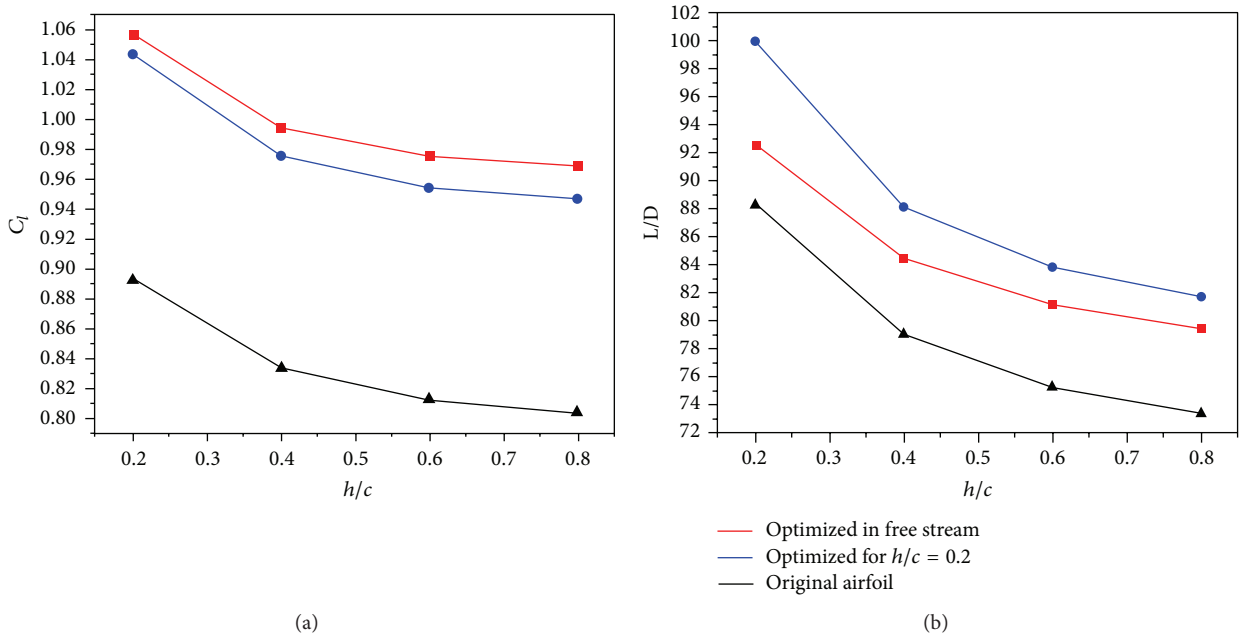

FIGURE 6: (a) Comparison of lift coefficient of the optimized airfoil in ground effect with height above the ground $h/c = 0.2$, the airfoil optimized in free-steam, and the original NACA 4412 airfoil for various ground heights h/c. (b) Comparison of lift to drag ratio of the airfoil optimized for free-stream condition and airfoil optimized in ground effect (with height above the ground $h/c = 0.2$) with that of the original NACA 4412 airfoil for various ground heights h/c.

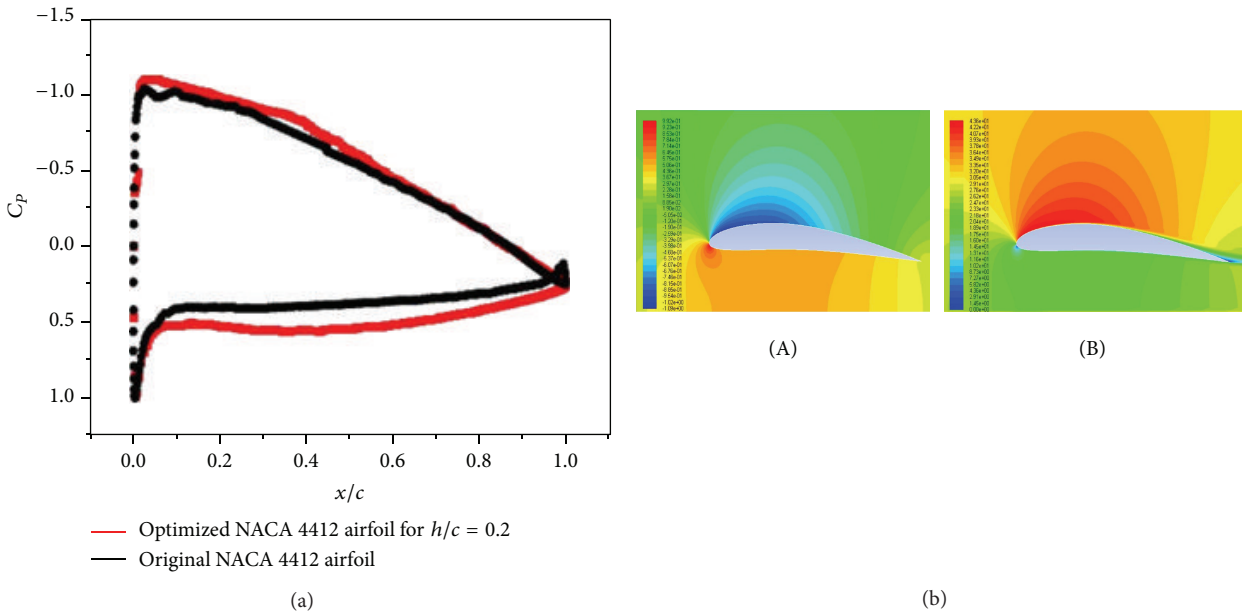

FIGURE 7: (a) Comparison of pressure coefficients between the optimized airfoil for $h/c = 0.2$ and the original airfoil in ground effect for height above the ground $h/c = 0.2$. (b) Contours of (A) pressure and (B) velocity around the airfoil optimized for $h/c = 0.2$ for height above the ground $h/c = 0.2$.

sampling; that is, the probability of selecting some individual h_i for reproduction is given by

$$P[h_i] = \frac{\text{fitness}(h_i)}{\sum_j \text{fitness}(h_j)}. \quad (1)$$

A crossover function is then performed to produce the offspring. Generally, crossover is implemented by choosing a crossover point on each individual and swapping alleles—or vector elements as illustrated in Figure 1.

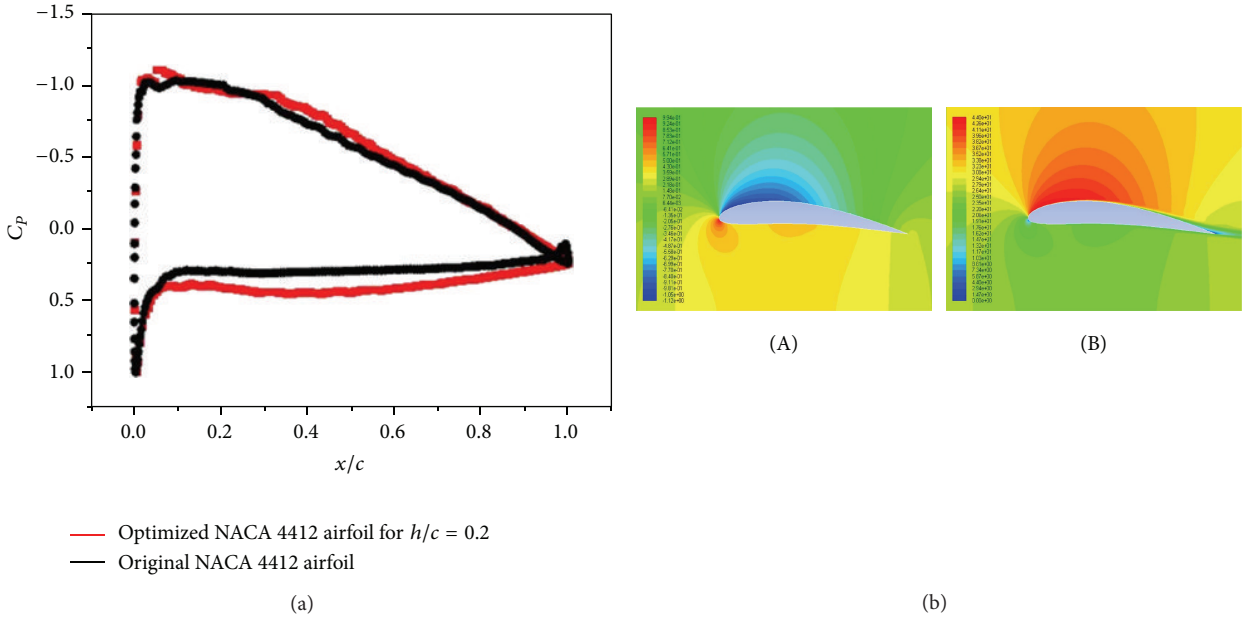

FIGURE 8: (a) Comparison of pressure coefficients between the optimized airfoil for $h/c = 0.2$ and the original airfoil in ground effect for height above the ground $h/c = 0.4$. (b) Contours of (A) pressure and (B) velocity around the airfoil optimized for $h/c = 0.2$ for height above the ground $h/c = 0.4$.

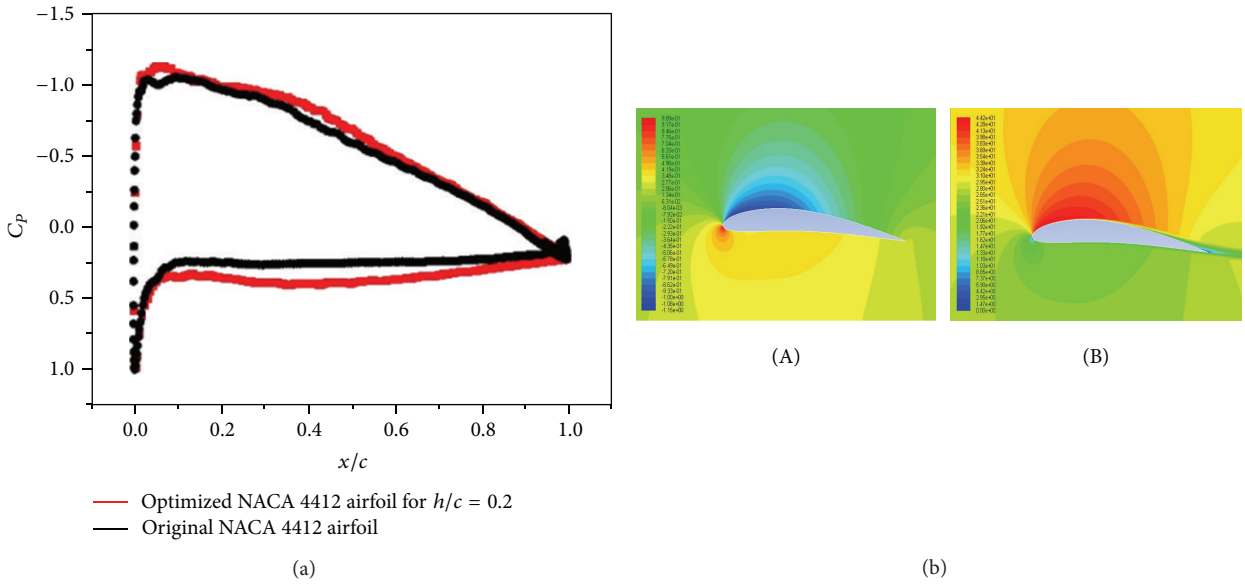

FIGURE 9: (a) Comparison of pressure coefficients between the optimized airfoil for $h/c = 0.2$ and original airfoil in ground effect for height above the ground $h/c = 0.6$. (b) Contours of (A) pressure and (B) velocity around the airfoil optimized for $h/c = 0.2$ for height above the ground $h/c = 0.6$.

(5) *Mutation*: randomly alter some small percentage of the population.

(6) *Check for Convergence*: if the solution has converged, return the best individual observed. If the solution has not yet converged, label the new generation as the current generation and go to Step (2). Convergence occurs after a certain number of generations when the shape of the optimized airfoil does not change from one generation to next.

2.2. Multiobjective Genetic Algorithm (MOGA). For many design problems, it is desirable to achieve, if possible, simultaneous optimization of multiple objectives [14]. These objectives, however, are usually conflicting, preventing simultaneous optimization of each objective [15]. Therefore, instead

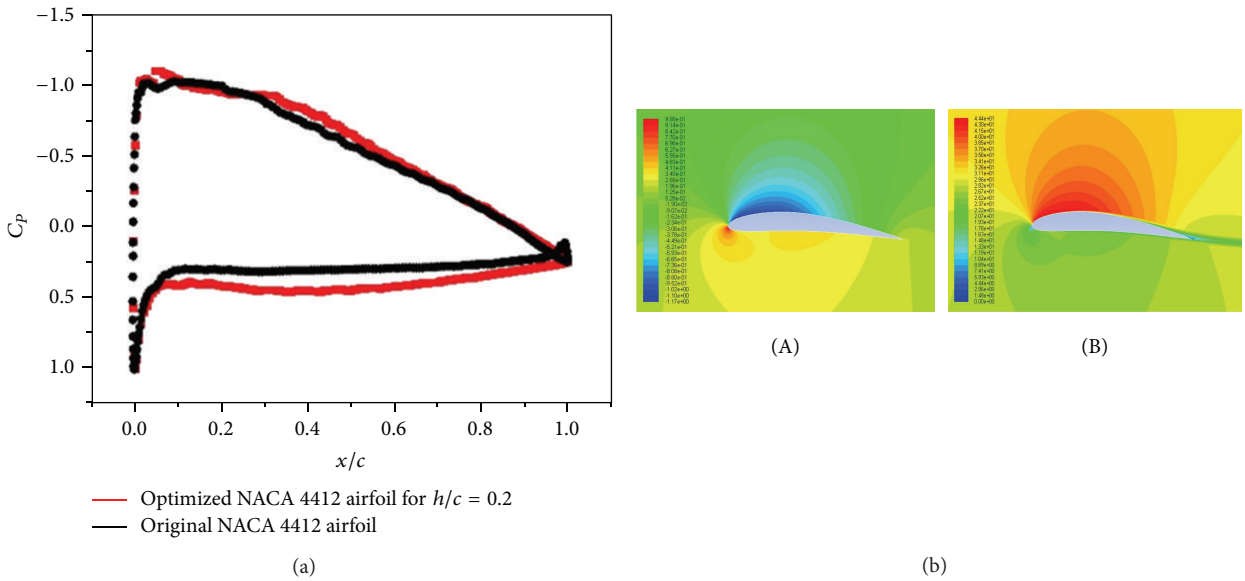

FIGURE 10: (a) Comparison of pressure coefficients between the optimized airfoil for $h/c = 0.2$ and original airfoil in ground effect for height above the ground $h/c = 0.8$. (b) Contours of (A) pressure and (B) velocity around the airfoil optimized for $h/c = 0.2$ for height above the ground $h/c = 0.8$.

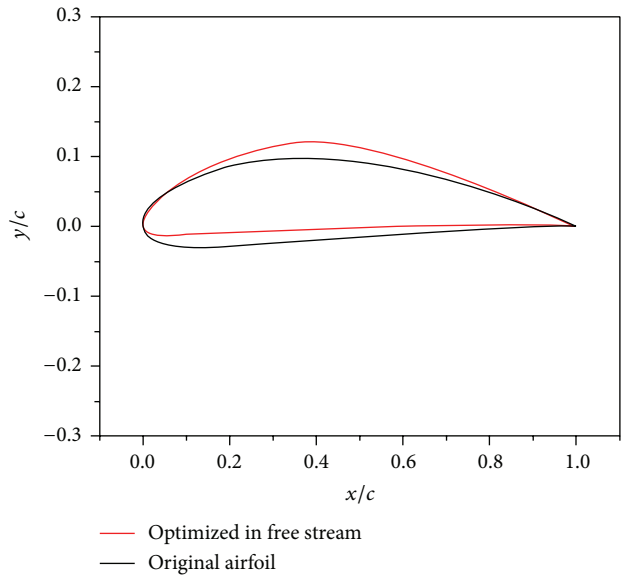

FIGURE 11: Comparison of shapes between the optimized airfoil and the original airfoil in free stream.

of searching for a single optimal solution, a multiobjective genetic algorithm (MOGA) is necessary to find a set of optimal solutions (generally known as Pareto-optimal solutions). For Pareto-optimal solutions, any individual inside the set dominates any individual outside the set while any individual in the set is not dominated by another individual in this solution set. The MOGA algorithms used to find the Pareto-optimal solutions to the airfoil optimization problem in this study are widely known as NSGA-II. It has the following three features: (1) it uses an elitist principle, (2) it uses an explicit diversity preserving mechanism, and (3) it emphasizes nondominated solutions in a population [16]. The implementation procedure of NSGA-II is as follows [17].

(1) *At 0th generation*: a random parent population P_0 of size N is created; it is sorted based on the nondomination. Then, the individuals in P_0 are ranked: 1 is the best level, 2 is the next-best level, and so on. Then, P_0 is sent to selection, recombination, and mutation operators to create off-spring population Q_0 of size N.

(2) *At tth generation*: a combined population $R_t = P_t U Q_t$ of size $2N$ is formed and is sorted according to nondomination. Then, individuals in R_t are divided into the best nondominated set F_1, the next-best nondominated set F_2 and so on. If the size of F_1 is smaller than N, all members of F_1 go to P_{t+1}, with the remaining members chosen from F_2, F_3,... until the size of P_{t+1} is N. Then, new population P_{t+1} is sent to selection, crossover, and mutation operators to create a new population Q_{t+1} of size N.

(3) *Termination*: the procedure terminates when convergence criterion is met.

The java code package utilized in this study is called jMetal. It is a Java-based framework for multiobjective optimization using metaheuristics. It is easy to use and is flexible and extensible [18].

2.3. Airfoil Parameterization. The airfoil shapes are parameterized using Bezier curves. Bezier curves are parametric curves frequently used in computer graphics and related fields. A Bezier curve is defined by a set of Bezier control points. Each curve can be expressed as polynomial equations containing the information of Bezier control points. The

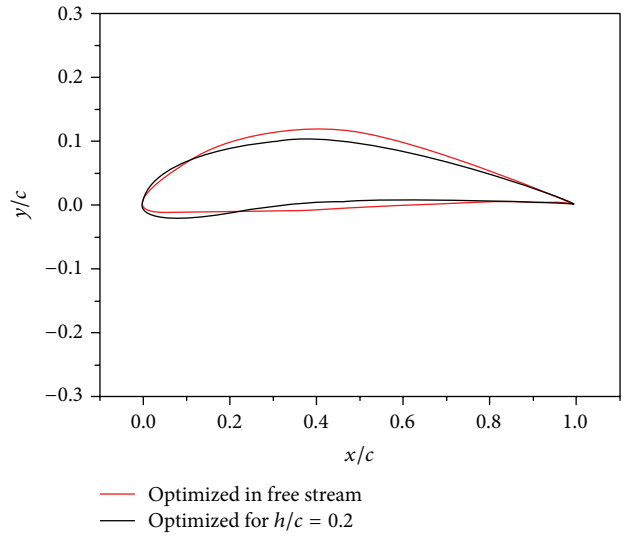

Figure 12: Comparison of shapes between airfoil optimized in free stream without ground effect with airfoil optimized in ground effect with height above the ground $h/c = 0.2$.

number of control points required to parameterize a curve depends on the shape of the curve.

Each airfoil is divided into top and bottom boundary curves by the airfoil chord joining its leading edge and the trailing edge. Considering the shape complexity of NACA 4412 airfoil, 12 control points are used for parameterization. For an airfoil curve, two points are fixed since they represent the leading and trailing edge of the airfoil. The intermediate points are allowed to move within the specified boundaries. A maximum thickness constraint of 16%-17% is used on the NACA 4412 airfoil. The constraints applied to the Bezier control points on the upper boundary of the airfoil are given as (x_i, y_i) and at the lower boundary of the airfoil as (m_i, n_i), $i = 1, 2 \ldots 6$, in Table 1.

Table 1: Coordinates of the control points used in airfoil parameterization.

		Upper limit	Lower limit			Upper limit	Lower limit
Top boundary	x_1	0.0054	0.0050	Bottom boundary	m_1	0.0012	0.0010
	x_2	0.040	0.038		m_2	0.042	0.040
	x_3	0.296	0.294		m_3	0.271	0.269
	x_4	0.367	0.365		m_4	0.411	0.410
	x_5	0.452	0.450		m_5	0.394	0.393
	x_6	0.817	0815		m_6	0.764	0.762
	y_1	0.016	0.014		n_1	−0.012	−0.018
	y_2	0.095	0.093		n_2	−0.020	−0.026
	y_3	0.113	0.111		n_3	0.005	0.0011
	y_4	0.149	0.147		n_4	−0.015	−0.03
	y_5	0.159	0.157		n_5	0.010	0.014
	y_6	0.049	0.047		n_6	0.0061	0.0066

3. The Shape Optimization Process for NACA 4412 Airfoil

This section presents the optimization process for NACA 4412 airfoil using the multiobjectives genetic algorithm (MOGA). An optimization procedure is established by coupling the MOGA code with the mesh generation code ANSYS ICEM and the CFD solver ANSYS FLUENT as shown in Figure 2.

The individuals in each generation of GA are represented by a set of control points, which generate the airfoil shape through the Bezier Curve. The mesh around the airfoil shape is generated using the grid generation software ANSYS ICEM, which is used to create a two-dimensional structured or unstructured mesh as an input to the CFD solver FLUENT. FLUENT is used to calculate the flow field for given flow conditions. Using the flow field data, FLUENT calculates the lift coefficient C_l and the drag coefficient C_d which are used to calculate the objective values for a given airfoil shape. Using the information about the objective values for all the airfoils in a given generation, MOGA is applied to create a next generation of airfoils and the process is repeated to obtain the Pareto front following the MOGA procedure outlined in Section 2. From the Pareto front, optimal solution for objective values is obtained. The airfoil shape that corresponds to the optimal objective values is the final shape of the optimized airfoil [17].

3.1. Implementation of MOGA. NSGA-II [17] and the jMetal [18] multiobjective GA software packages are employed. We choose 20 individuals (airfoils) for each generation. The crossover rate of 0.9 is considered. The mutation rate is determined to be 1/24. jMetal MOGA framework offers multiple operators; here we employ the simulated binary crossover (SBX) operator and the polynomial mutation operator for crossovers and mutations, respectively. The selection process employs the binary tournament operator.

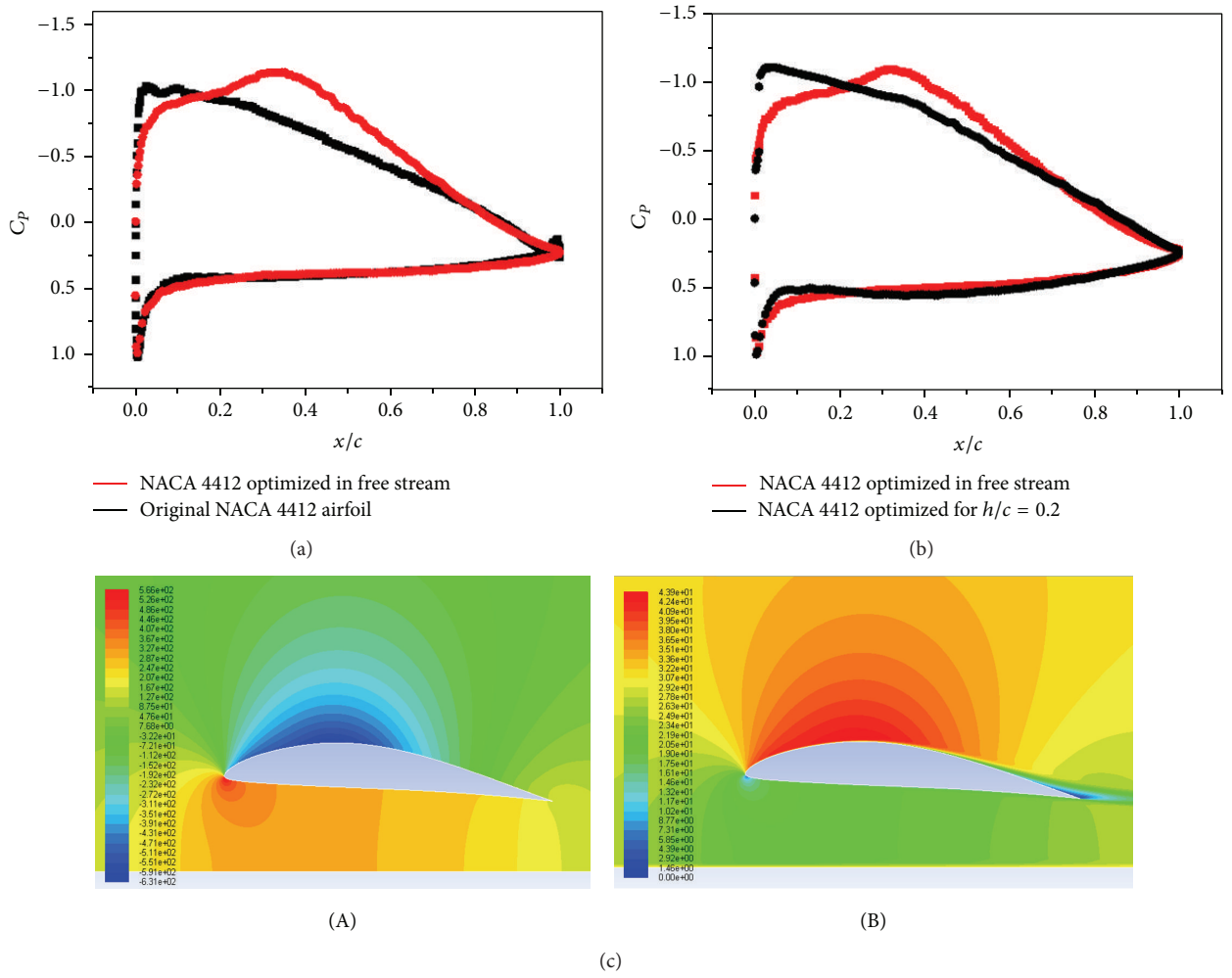

Figure 13: (a) Comparison of pressure coefficients between airfoil optimized in free stream and the original airfoil in free stream. (b) Comparison of pressure coefficients under free steam condition between airfoil optimized in free stream without ground effect and the airfoil optimized in ground effect with $h/c = 0.2$. (c) Contours of (A) pressure and (B) velocity around the optimized airfoil (optimized in ground effect for $h/c = 0.2$) under free stream condition.

The multiobjective optimization procedure is conducted with two objectives functions. The first objective is to minimize $10/C_l$, and the second objective is to minimize $100 * C_d/C_l$. The goal is to find the Pareto front for these two objective functions. When the value of both objective functions does not change from one generation to the next, the solution is considered converged to an optimal value of C_l and C_l/C_d. The airfoil shape that corresponds to the optimal objective values is the final shape of the optimized airfoil.

3.2. Mesh Generation. The commercially available software ICEM is used to generate a structured mesh around NACA 4412 airfoil. Adaptive meshing is employed. A reply file is scripted to automatically generate mesh around different airfoils in a given generation. The reply file is edited so as to be able to generate mesh based on different airfoil shapes. Figure 3 shows the structured mesh around NACA 4412 airfoil. Approximately 50305 quadrilateral cells exist in this mesh in Figure 3. The ground is treated as a moving wall boundary.

Grid independence is assessed by establishing another finer mesh. The number of quadrilateral elements is doubled in the finer mesh. The height of the first layer element in finer mesh is halved from the original mesh. The y^+ value for any mesh point next to the wall never exceeds 2. Results show that the variation in lift coefficient on the coarse and fine mesh is very small; the coarse mesh gives acceptable results. Therefore, the original mesh is adopted in the calculations given in this paper for the reasons of computational efficiency with acceptable accuracy.

3.3. Flow Field Computations. The numerical simulations are performed using FLUENT 14.5. A journal file is written for autorunning of FLUENT in the MOGA optimization process.

For NACA 4412 airfoil in ground effect, the typical flow condition is free stream velocity $V_\infty = 30.8$ m/s with corresponding Reynolds number based on chord length Re

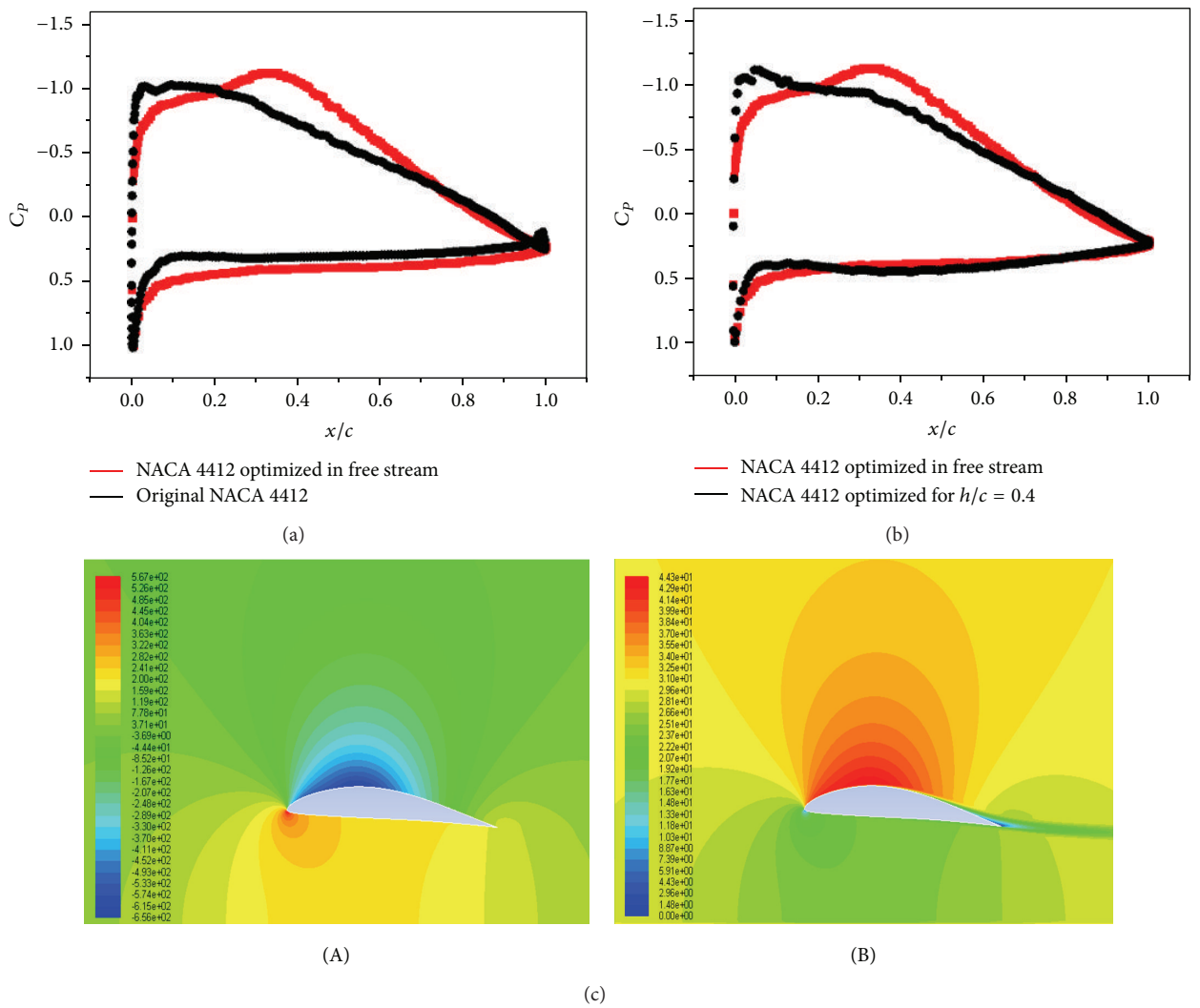

FIGURE 14: (a) Comparison of pressure coefficients between airfoil optimized in free steam and the original airfoil at $h/c = 0.4$. (b) Comparison of pressure coefficients between the optimized airfoil (optimized for $h/c = 0.2$) and the airfoil optimized in free stream at $h/c = 0.4$. (c) Contours of (A) pressure and (B) velocity around the airfoil optimized in free stream at $h/c = 0.4$.

$= 3 \times 10^5$. In the flow field simulation, the Cartesian frame of reference is fixed to the initial position of the airfoil.

In the flow field computation, compressible Reynolds-Averaged Navier-Stokes (RANS) equations are employed. One equation Spalart-Allmaras (S-A) model is chosen for turbulence modeling. The governing equations are solved using the finite-volume solver in ANSYS FLUENT; convection terms and diffusion terms are discretized with second-order upwind scheme and central difference scheme, respectively. The pressure-based solver is used with SIMPLEC scheme to address the pressure-velocity coupling.

In order to evaluate the accuracy of the numerical method for predicting the flow field and aerodynamic forces on an airfoil in ground effect, the flow field of a Tyrrell-026 airfoil in static ground effect (SGE) is simulated and compared with the wind tunnel experiment data [19]. Figure 4 shows the excellent comparison between the pressure coefficient distribution from our CFD simulations and the experimental data.

4. Results and Discussion

We choose ground clearance of $0.2c$ (0.2∗Chord Length) and angle of attack of 4 degrees for optimization of NACA 4412 airfoil. The free stream velocity is taken as 30.8 m/s. This is a typical operating condition for wing in ground effect (WIG) craft in the proximity of the ground. For airfoil optimization, we set two optimization objectives, that is to minimize $10/C_l$ as well as $100 * C_d/C_l$. The airfoil shape that results in lowest value of $100 * C_d/C_l$ in the Pareto front gives the shape of the optimized airfoil. Figure 5 shows the shape comparison of optimized NACA 4412 airfoil with $h/c = 0.2$ with the original airfoil. The optimized NACA 4412 airfoil with $h/c = 0.2$

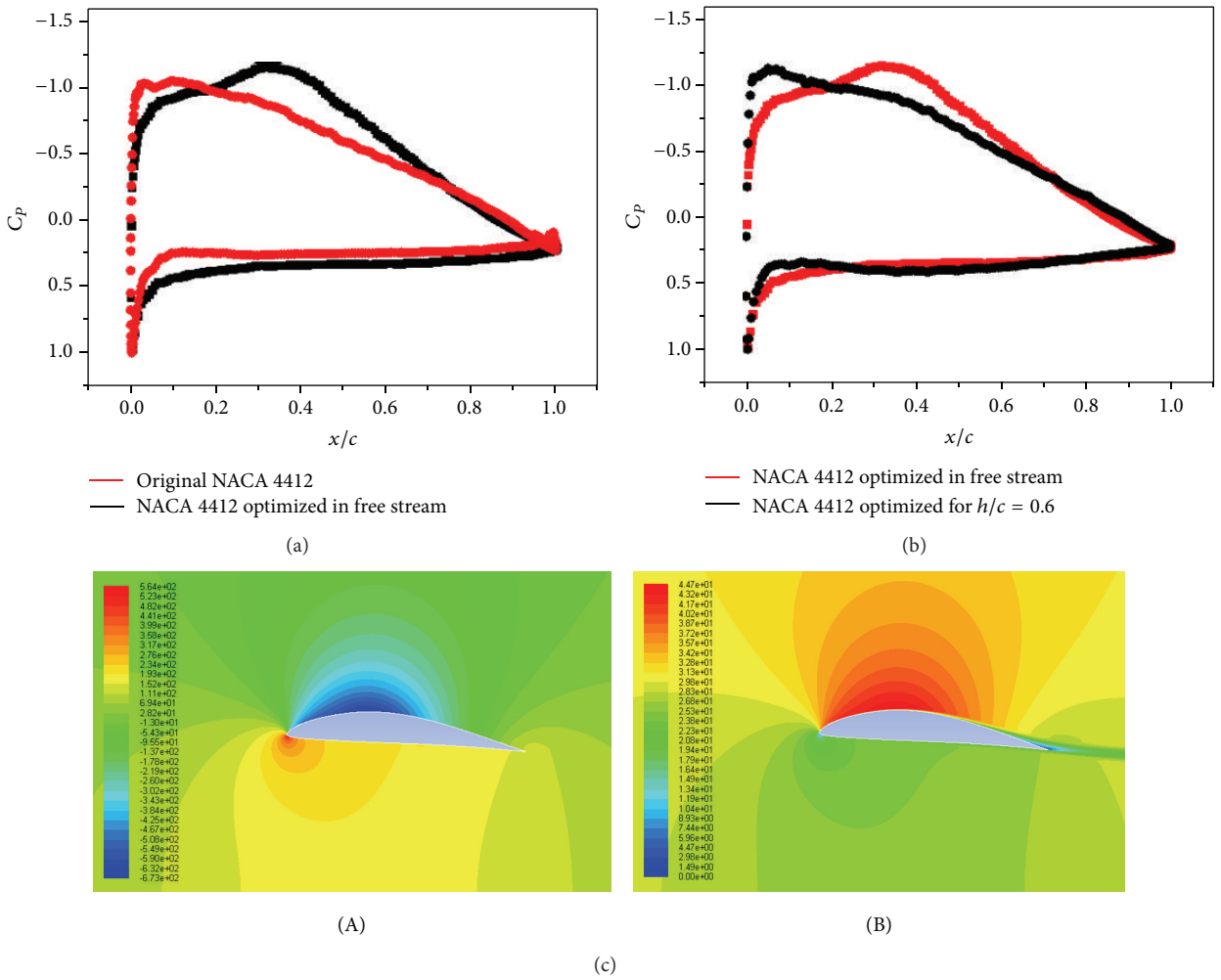

FIGURE 15: (a) Comparison of pressure coefficients between airfoil optimized in free steam and the original airfoil at $h/c = 0.6$. (b) Comparison of pressure coefficients between the airfoil (optimized for $h/c = 0.2$) and the airfoil optimized in free stream at $h/c = 0.6$. (c) Contours of (A) pressure and (B) velocity around the airfoil optimized in free stream at $h/c = 0.6$.

is simulated for three other ground clearances (0.4c, 0.6c, and 0.8c), comparing its lift coefficient and lift to drag ratio with original NACA 4412 airfoil and the airfoil optimized in free stream without ground effect. The results in Figure 6 show that the optimized airfoil for $h/c = 0.2$ has an overall better performance than the original airfoil for both the aerodynamic properties—the lift coefficient and lift to drag ratio. Figures 7, 8, 9, and 10 show the comparison of pressure coefficient between the airfoil optimized for $h/c = 0.2$ and the original NACA 4412 airfoil and the contours of pressure coefficient and velocity magnitudes around the optimized airfoil optimized for $h/c = 0.2$ at ground heights of 0.2c, 0.4c, 0.6c, and 0.8c, respectively.

To prove the necessity of optimizing an airfoil for wing in ground effect (WIG) craft, we also optimized the NACA 4412 airfoil without ground effect. Figures 11 and 12, respectively, show the shape comparison of the optimized airfoil without ground effect with the original airfoil and with the optimized airfoil in ground effect with 0.2c height above the ground.

As discussed before, the flow field past the optimized airfoil without ground effect is simulated under four ground effect heights of 0.2c, 0.4c, 0.6c, and 0.8c. The lift coefficient and lift to drag ratio for these four heights are compared with those of the airfoil optimized in ground effect for height 0.2c above the ground. Figure 6(b) and Table 2 show that the airfoil optimized in ground effect for height 0.2c above the ground has a higher lift to drag ratio than the airfoil optimized without ground effect. This implies that the airfoil optimized in ground effect has a higher aerodynamic efficiency than the one optimized without ground effect. Therefore, it is useful to design an airfoil specifically suited for wing in ground effect craft under take-off condition.

Figures 13, 14, 15, and 16, respectively show the comparison of (a) pressure coefficients between the airfoil optimized in free-stream and the original airfoil, (b) pressure coefficients between the airfoil (optimized for $h/c = 0.2$) and the airfoil optimized in the free stream, and (c) The contours of pressure and velocity around the airfoil optimized in free-stream at $h/c = 0.2$, 0.4, 0.6 and 0.8.

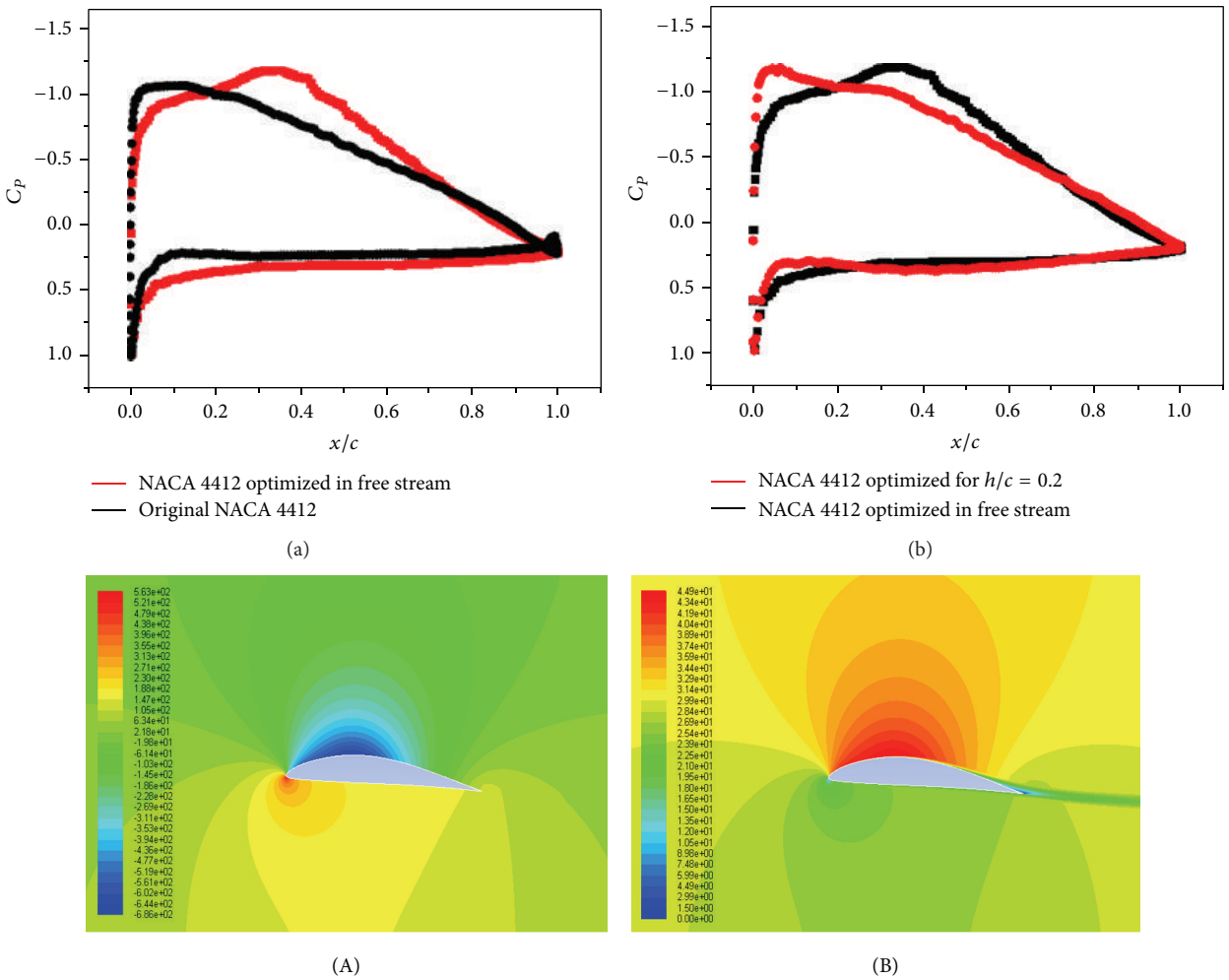

Figure 16: (a) Comparison of pressure coefficients between the airfoil optimized in free stream and the original airfoil at $h/c = 0.8$. (b) Comparison of pressure coefficients between the airfoil (optimized for $h/c = 0.2$) and the airfoil optimized in free stream at $h/c = 0.8$. (c) Contours of (A) pressure and (B) velocity around the airfoil optimized in free stream at $h/c = 0.8$.

Table 2: Lift to drag ratio (L/D) for original and optimized NACA 4412 airfoil in ground effect for various heights above the ground.

h/c	L/D of original airfoil	L/D of airfoil optimized for $h/c = 0.2$	L/D of airfoil optimized in free stream without ground effect
0.2	88.32	99.96	92.56
0.4	79.01	88.13	84.50
0.6	75.28	83.87	81.21
0.8	73.35	81.71	79.50

5. Conclusions

In this paper, we have employed a multiobjective genetic algorithm (MOGA) to optimize the shape of a well-known wing in ground effect (WIG) craft airfoil—the NACA 4412—to improve its lift and drag characteristics, in particular to achieve two objectives that is to increase its lift as well as its lift to drag ratio. The commercially available software FLUENT is employed to calculate the flow field on an adaptive structured mesh using the Reynolds-Averaged Navier-Stokes (RANS) equations in conjunction with a one equation Spalart-Allmaras (S-A) turbulence model. The results show significant improvement in both the lift coefficient and the lift to drag ratio of the optimized airfoil compared to the original airfoil. The results are obtained for optimized airfoils in ground effect for various heights above the ground. The results demonstrate the importance of using airfoils optimized in ground effect under take-off conditions of a WIG aircraft.

Conflict of Interests

The authors declare that there is no conflict of interests regarding the publication of this paper.

References

[1] M. Halloran and S. O. Meara, "Wing in ground effect craft review," Tech. Rep. CR-9802, Sir Lawrence Wackett Centre for Aerospace Design Technology, Royal Melbourne Institute of Technology, Melbourne, Australia, 1999.

[2] K. Rozhdestvensky, *Aerodynamics of a Lifting System in Extreme Ground Effect*, Springer, 2000.

[3] L. Yun, A. Bliault, and J. Doo, *WIG Craft and Ekranoplan: Ground Effect Craft Technology*, Springer, New York, NY, USA, 2010.

[4] G. Doig and T. J. Barber, "Considerations for numerical modeling of inverted wings in ground effect," *AIAA Journal*, vol. 49, no. 10, pp. 2330–2333, 2011.

[5] M. R. Ahmed, T. Takasaki, and Y. Kohama, "Aerodynamics of a NACA4412 airfoil in ground effect," *AIAA Journal*, vol. 45, no. 1, pp. 37–47, 2007.

[6] S. Mahon and X. Zhang, "Computational analysis of pressure and wake characteristics of an aerofoil in ground effect," *Journal of Fluids Engineering, Transactions of the ASME*, vol. 127, no. 2, pp. 290–298, 2005.

[7] D. F. Wang and C. Dai, "Experimental research on the aerodynamics of a symmetrical airfoil near free surface," *Journal of Fluids Engineering*, vol. 127, no. 2, pp. 290–298, 2005.

[8] S.-H. Lee and J. Lee, "Optimization of three-dimensional wings in ground effect using multiobjective genetic algorithm," *Journal of Aircraft*, vol. 48, no. 5, pp. 1633–1645, 2011.

[9] X. Zhang and J. Zerihan, "Edge vortices of a double-element wing in ground effect," *Journal of Aircraft*, vol. 41, no. 5, pp. 1127–1137, 2004.

[10] Y. Zhigang and Y. Wei, "Complex flow for wing-in-ground effect craft with power augmented ram engine in cruise," *Chinese Journal of Aeronautics*, vol. 23, no. 1, pp. 1–8, 2010.

[11] X. G. Qin, *Numerical simulation of high lift device in ground effect [Ph.D. thesis]*, Beijing University of Aeronautics and Astronautics, Beijing, China, 2010.

[12] D. E. Goldberg, *Genetic Algorithms in Search, Optimization, and Machine Learning*, Addison-Wesley, New York, NY, USA, 1989.

[13] B. Morgan, "Gairfoils: finding high-lift Joukowski airfoils with a genetic algorithm," Tech. Rep., Department of Mechanical Engineering, Washington University, St. Louis, MO, USA, 2007.

[14] N. Srinivas and K. Deb, "Muiltiobjective optimization using nondominated sorting in genetic algorithms," *Evolutionary Computation*, vol. 2, no. 3, pp. 221–248, 1994.

[15] A. Konak, D. W. Coit, and A. E. Smith, "Multi-objective optimization using genetic algorithms: a tutorial," *Reliability Engineering & System Safety*, vol. 91, no. 9, pp. 992–1007, 2006.

[16] K. Deb, "Single and multi-objective optimization using evolutionary computation," in *Proceedings of the 6th International Conference on Hydro-Informatics*, pp. 14–35, Singapore, 2004.

[17] K. Deb, A. Pratap, S. Agarwal, and T. Meyarivan, "A fast and elitist multiobjective genetic algorithm: NSGA-II," *IEEE Transactions on Evolutionary Computation*, vol. 6, no. 2, pp. 182–197, 2002.

[18] J. J. Durillo, A. J. Nebro, and E. Alba, "The jMetal framework for multi-objective optimization: design and architecture," in *Proceedings of the IEEE Congress on Evolutionary Computation (CEC'10)*, pp. 4138–4325, July 2010.

[19] S. Mahon and X. Zhang, "Computational analysis of pressure and wake characteristics of an aerofoil in ground effect," *Journal of Fluids Engineering*, vol. 127, no. 2, pp. 290–298, 2005.